Developmental Biology **250,** 145–155 (2002)
doi:10.1006/dbio.2002.0785

Caenorhabditis elegans Cell Migration and Axon Outgrowth

Yi-Chun Wu,[1] Ting-Wen Cheng, Ming-Chia Lee, and Nei-Ying Weng

Department of Zoology, National Taiwan University, No1 Sec4 Roosevelt Road, Taipei 10617 Taiwan

Rac GTPases act as molecular switch in various morphogenic events. However, the regulation of their activities during the development of multicellular organisms is not well understood. *Caenorhabditis elegans* rac genes *ced-10* and *mig-2* have been shown to act redundantly to control P cell migration and the axon outgrowth of D type motoneurons. We showed that *ced-10* and *mig-2* also control amphid axon outgrowth and amphid dendrite fasciculation in a redundant fashion. Our biochemical and genetic data indicate that *unc-73,* which encodes a protein related to Trio-like guanine nucleotide exchange factor, acts as a direct activator of *ced-10* and *mig-2* during P cell migration and axon outgrowth of D type motoneurons and amphid sensory neurons. Furthermore, rac regulators *ced-2*/crkII and *ced-5*/dock180 function genetically upstream of *ced-10* and *mig-2* during axon outgrowth of D type motoneurons and act upstream of *mig-2* but not *ced-10* during P cell migration. However, neither *ced-2*/crkII nor *ced-5*/dock180 is involved in amphid axon outgrowth. Therefore, distinct rac regulators control *ced-10* and *mig-2* differentially in various cellular processes.

Key Words: **axon outgrowth; cell migration; guanine nucleotide exchange factor; rac; *ced-2*; *ced-5*; *ced-10*; *ced-12*; *mig-2*; *unc-73*.**

INTRODUCTION

Members of the Rho-like small GTPase family (Rho, Rac, and Cdc42) are important regulators of cytoskeleton and cell-shape change (Hall, 1998; Settleman, 2001). In mammalian fibroblasts, RhoA regulates the formation of specific actin-based structures, called stress fiber, whereas Rac and Cdc42 control the formation of lamellipodia and filopodia, respectively (Hall, 1998). Rho, Rac, and Cdc42 cycle between an inactive GDP-bound state and an active GTP-bound state. The activity of GTPases is determined by the ratio of their GTP/GDP-bound forms in the cell. The ratio of the two forms is controlled by three classes of regulatory proteins (D'Souza-Schorey *et al.*, 1997; Kaibuchi *et al.*, 1999). Guanine nucleotide exchange factors (GEFs) stimulate the exchange of bound GDP for GTP and therefore convert GTPases to an active form. GTPase-activating proteins (GAPs) increase the intrinsic rate of hydrolysis of bound GTP and facilitate inactivation of GTPases. Guanine nucleotide dissociation inhibitors (GDIs) bind to the GDP form of GTPases and prevent GDP release, and hence promote the inactive state of the protein.

The genome of *Caenorhabditis elegans* contains three rac-like genes: *ced-10* (*rac-1*), *rac-2*, and *mig-2* (Lundquist *et al.*, 2001). There are mutations in both *ced-10* and *mig-2* loci. Loss-of-function (lf) mutations in *ced-10* cause defects in the migration pattern of distal tip cells (DTCs) and the phagocytosis of apoptotic cells (Reddien and Horvitz, 2000). *mig-2*(gain-of-function, gf) mutants are uncoordinated and defective in migrations of many cells (Zipkin *et al.*, 1997). Interestingly, *mig-2*(lf) mutants move normally and are defective in only a small subset of cell migrations. These observations suggest that, in many cells, the *mig-2*(gf) mutations exert their effects by interfering with processes in which *mig-2* itself is not required, possibly by competing with functionally redundant Rho family members (Zipkin *et al.*, 1997). Alternatively, *mig-2*(gf) mutations may have neomorphic effects on a process in which *mig-2* normally participates. Genetic studies suggest that *ced-10* and *mig-2* act redundantly to control several developmental processes, including CAN axon guidance, the phagocytosis of apopto-

[1] To whom correspondence should be addressed. Fax: (886) 2-2363-6837. E-mail: yichun@ccms.ntu.edu.tw.

0012-1606/02 $35.00

tic cells, and the migration of DTCs, P cells, and CAN cells (Lundquist *et al.*, 2001; Spencer *et al.*, 2001). All of these cellular processes require rearrangement of actin filaments to produce cellular protrusions in response to extracellular signals. Previous studies showed that *ced-2*, *ced-5*, and *ced-12*, which encode proteins related to human CrkII, DOCK180, and ELMO, respectively, act genetically upstream of *ced-10* to regulate the phagocytosis of apoptotic cells and the migration of DTCs (Wu and Horvitz, 1998; Reddien and Horvitz, 2000; Gumienny *et al.*, 2001;Wu *et al.*, 2001; Zhou *et al.*, 2001). *ced-10* and *mig-2* have been shown to act cell-autonomously in migrating cells and neurons to control cell migration and axon outgrowth, respectively (Reddien and Horvitz, 2000, Lundquist *et al.*, 2001). However, pathways that couple extracellular signals to *ced-10* and *mig-2* to control axon outgrowth and cell migration are not well characterized.

unc-73 encodes a Dbl homology GEF (DH-GEF) protein related to Trio and interacts with *ced-10* and *mig-2* during CAN axon guidance and the migration of DTCs, P cells, and CAN cells (Steven *et al.*, 1998; Lundquist *et al.*, 2001; Spencer *et al.*, 2001). Despite the fact that biochemical studies showed that *Drosophila* and human Trios, which also function in axonal development, possess a GEF activity for RAC *in vitro* (Debant *et al.*, 1996; Awasaki *et al.*, 2000; Liebl *et al.*, 2000; Newsome *et al.*, 2000; O'Brien *et al.*, 2000), no direct evidence thus far shows that UNC-73 is able to stimulate guanine nucleotide exchange in CED-10 or MIG-2.

In this report, we showed that UNC-73 has a guanine nucleotide exchange activity for both CED-10 and MIG-2 *in vitro*. We examined the roles and relationships of *ced-10*, *mig-2*, and *unc-73* during the development of D type motoneurons and amphid sensory neurons. Furthermore, we investigated whether CED-2/CRKII, CED-5/DOCK180, and CED-12/ELMO function as rac regulators during the development of D type motoneurons and amphid sensory neurons.

MATERIALS AND METHODS

Nematodes

C. elegans strains were grown at 20°C, except where otherwise noted. All mutations were generated in a strain Bristol N2 background, the standard wild-type strain (Brenner, 1974). The following mutations were used: LG I: *unc-73(e936, gm33, rh40)*, *ced-12(n3261, tp2)*; LG III: *juls73*[*unc-25::gfp*]; LG IV: *ced-2(e1752, n1994)*, *ced-5(n1812, n2002)*, *ced-10(n1993, n3246)*; LG X: *mig-2(gm38, mu28)*, *lon-2(e678)*.

Analysis of D Type Motoneurons

The *juls73(unc-25::gfp)* integrated transgene (kindly provided by Y. Jin) was introduced to various genetic backgrounds to visualize axons and cell bodies of D-type motoneurons. Young adults of transgenic worms were picked and observed by using fluorescence microscopy. In the wild-type strain carrying the *unc-25::gfp* transgene, all cell bodies of DDs and VDs are located in the ventral cord as normal, and approximately 5 and 8% of animals showed branching and premature termination in a single commissure of D-type neurons, respectively.

Analysis of Amphid Neurons

To visualize the amphid neurons, animals were stained with DiO as previously described (Hedgecock *et al.*, 1985; Herman and Hedgecock, 1990). Briefly, young adult worms were incubated in 10 μg/ml DiO (Molecular Probes) solution for 2–3 h, washed three times with M9, and allowed to recover on plates for more than 30 min. Worms were then observed by using fluorescence microscopy.

Analysis of P Cell Migration

Mutants without misplaced VD neurons were scored as normal for P cell migration. For mutants with lateral VD neurons, L2 animals were mounted on slides with 3 mM sodium azide, and their P1.p through P12.p in the ventral cord were examined using Nomarski optics. Typically, a lateral VD neuron was accompanied with ectopic neurons in the neighborhood, which are likely derived from the same P cell that did not undergo ventral migration, and the corresponding Pn.p nucleus was missing in the ventral cord.

Transcriptional Overexpression

Generation of the P_{hsp}*::ced-10(V12)* constructs has been previously described (Wu *et al.*, 2001). P_{hsp}*::ced-10(V12)* was coinjected with *myo-2::gfp* to generate stable lines. To test for the transgene effect on DD axon outgrowth, eggs laid for 3 h were subject to a 2.5-min heatshock treatment at 33°C. Young transgenic L1 larvae were scored for the rescue of DD axon outgrowth. To test the transgene effect on P cell migration, eggs laid for 11 h were subject to a 2.5-min heatshock treatment at 33°C. Young transgenic adults were scored for lateral VDs.

Protein Production and Guanine Nucleotide Exchange Assay

The cDNA fragment corresponding to UNC-73 GEF1 (residues 1202–1423) was amplified by PCR from yk479h7 cDNA and cloned into the pMAL-c2 expression vector (New England Biolab) to express UNC-73GEF1-MBP (maltose binding protein) fusion protein. The *ced-10* and *mig-2* cDNA fragments were cloned to the pGEX-3X and pGEX4T-3 expression vectors (Ampharmacia) to express CED-10-GST (glutathione *S*-transferase) and MIG-2-GST fusion proteins, respectively. Fusion proteins were induced and purified according to manufacturers' protocols.

The GEF assay was performed as previously described with slight modification (Debant *et al.*, 1996; Hardt *et al.*, 1998). Briefly, [^{3}H]GDP-loaded GTPases were prepared by incubating 20 μg purified GTPase fusion proteins with 30 μl loading buffer (50 mM Tris–HCl, pH 7.5, 50 mM NaCl, 5 mM EDTA, 1 mM DTT, 10 μM [^{3}H]GDP, 40 μg/ml BSA) at 25°C for 20 min. After incubation, the reaction was terminated by adding 60 μl ice-cold buffer (50 mM Tris–HCl, pH 7.5, 10 mM $MgCl_2$, 1 mM DTT, 40 μg/ml BSA) and 5 μl 100 mM $MgCl_2$ and further incubated for 15 min at 25°C. For the GEF assay, purified UNC-73GEF1-MBP fusion protein (10 μg) and 20 μl each [^{3}H]GDP-loaded GTPase were mixed in an 80-μl reaction buffer (50 mM Tris–HCl, pH 7.5, 1 mM GTP, 2 mM

$MgCl_2$) at 25°C for 30 min. The reactions were quenched by adding termination buffer (50 mM Tris–HCl, pH 7.5, 10 mM $MgCl_2$) and immediately filtrated through a nitrocellulose membrane (BA85, 0.45 μm; Schleicher & Schuell). Filters were then washed with termination buffer three times, and the amount of radioactivity on the filters was determined.

Yeast Two-Hybrid Assay

The *ced-10*, *mig-2*, and *cdc-42* cDNA were cloned into pPC86 (Gibco) to produce AD fusion proteins, and the *unc-73* cDNA encoding the GEF1/SH3 region and the last spectrin-like repeat (residues 842-1634) was cloned into pDBLeu (Gibco) to produce DB fusion protein. In the yeast two-hybrid assay, specific pairs of constructs expressing AD and DB fusion proteins were transformed to the yeast strain MaV203 (Gibco). Transformants were selected on synthetic complete medium lacking tryptophan and leucine (SC-Trp-Leu). Individual colonies were streaked on SC-Trp-Leu-His in the presence of 3AT to test for the activation of the reporter gene *HIS3*.

RESULTS

ced-10 and mig-2 Act Redundantly in Genetic Pathways That Control the Development of D-Type Motoneurons and Amphid Sensory Neurons

ced-10(*n1993*);*mig-2*(*mu28*) double mutants are severely uncoordinated and nearly paralyzed. In contrast, *ced-10*(*n1993*) and *mig-2*(*mu28*) single mutants show normal locomotion on agar plates. The alleles *n1993* and *mu28* are partial loss-of-function and null, respectively (Zipkin *et al.*, 1997; Reddien and Horvitz, 2000). To better understand the redundant roles played by *ced-10* and *mig-2* during the development of the nervous system, we specifically analyzed D-type motoneurons and amphid sensory neurons in these mutants.

D-type motoneurons consisting of 6 DD neurons (which innervate the dorsal body muscles) and 13 VD neurons (which innervate the ventral body muscles) express GABA (γ-aminobutyric acid) neurotransmitter and cause muscle relaxation during locomotion (White *et al.*, 1986; McIntire *et al.*, 1993). DDs are generated and differentiate during embryogenesis, while VDs are born as descendents of P blast cells at the first larval stage. P cells that originally line up in a ventrolateral row on each side of animal migrate to the ventral cord where each P cell undergoes a few rounds of divisions to give rise to a hypodermal precursor cell Pn.p and a few neural descendents, including VD (Sulston, 1976). To facilitate our observation of D-type motoneurons, we utilized the integrated *unc-25::gfp* transgene that is specifically expressed in GABAergic neurons, including DDs and VDs (Jin *et al.*, 1999) (Fig. 1A). We found that *ced-10*(*n1993*); *mig-2*(*mu28*) double mutants exhibited approximately five laterally localized VD cell bodies, and such a defect was not observed in *ced-10*(*n1993*) or *mig-2*(*mu28*) single mutants (Fig. 1B, Table 1). To investigate whether the VD mislocalization phenotype of *ced-10*(*n1993*);*mig-2*(*mu28*) mutants was caused by the defect in P cell migration, we examined locations of descendents of the P blast cell that generated a lateral VD. We observed ectopic neurons near the misplaced VDs on the lateral side of animal and the absence of corresponding Pn.p nuclei in the ventral cord. Moreover, lateral vulvae generated by lateral Pn.p cells were frequently observed in adults (data not shown). Together, these observations indicate that lateral VDs observed in *ced-10*(*n1993*);*mig-2*(*mu28*) double mutants were generated by P cells that failed to undergo ventral migration, and these P cells, despite of a migration defect, still divided and differentiated normally.

Wild-type animals carrying the *unc-25::gfp* transgene showed GFP expression in approximately 17 DD and VD commissures (Fig. 1A). *ced-10*(*n1993*);*mig-2*(*mu28*) double mutants exhibited approximately 8 aberrant commissures that failed to reach the dorsal cord, resulting from pretermination, misrouting, or branching (Fig. 1B, Table 1). However, 54% of *ced-10*(*n1993*) mutants and 70% of *mig-2*(*mu28*) mutants displayed similar defects in approximately 2 commissures (Table 1). These results are consistent with the previous observation that *ced-10* and *mig-2* act redundantly during DDs and VDs commissure outgrowth (Lundquist *et al.*, 2001).

Besides D-type motoneurons, amphid, which is the primary nematode sensory organ and functions to detect chemicals, touch, and temperature, is also defective in *ced-10*;*mig-2* double mutants. Amphid consists of 12 bilaterally symmetric pairs of sensory neurons in the head region of animals (White *et al.*, 1986). Each amphid neuron extends 2 processes: 1 dendrite that runs anteriorly to the amphid sensillum and 1 axon that extends ventrally and enters the circumpharyngeal nerve ring. In the nerve ring, amphid sensory axons contact sensory and interneuron targets, establishing neural circuits essential to sensation and behavior (White *et al.*, 1986). To visualize amphid neurons in living worms, we treated worms with the fluorescent dye DiO that stains 6 bilaterally amphid neurons: ADF, ASH, ASI, ASJ, ASK, and ADL. We found that in *ced-10*(*n1993*);*mig-2*(*mu28*) double mutants, the amphid dendritic processes were frequently defasciculated and axon bundles entering the nerve ring were not observed (Fig. 2B, Table 1). In contrast, both *ced-10*(*n1993*) and *mig-2*(*mu28*) single mutants showed normal amphid axon outgrowth and amphid dendrite fasciculation. These results suggest that *ced-10* and *mig-2* act redundantly during amphid axon outgrowth and amphid dendrite fasciculation.

The First DH/PH Domain of UNC-73 Has a GEF Activity for Both CED-10 and MIG-2 in Vitro

UNC-73 has been shown to function in P cell migration through activation of RHO-1 and acts with CED-10 and MIG-2 during CAN axon pathfinding and CAN cell migration (Lundquist *et al.*, 2001; Spencer *et al.*, 2001). We observed lateral VD neurons and aberrant DD and VD

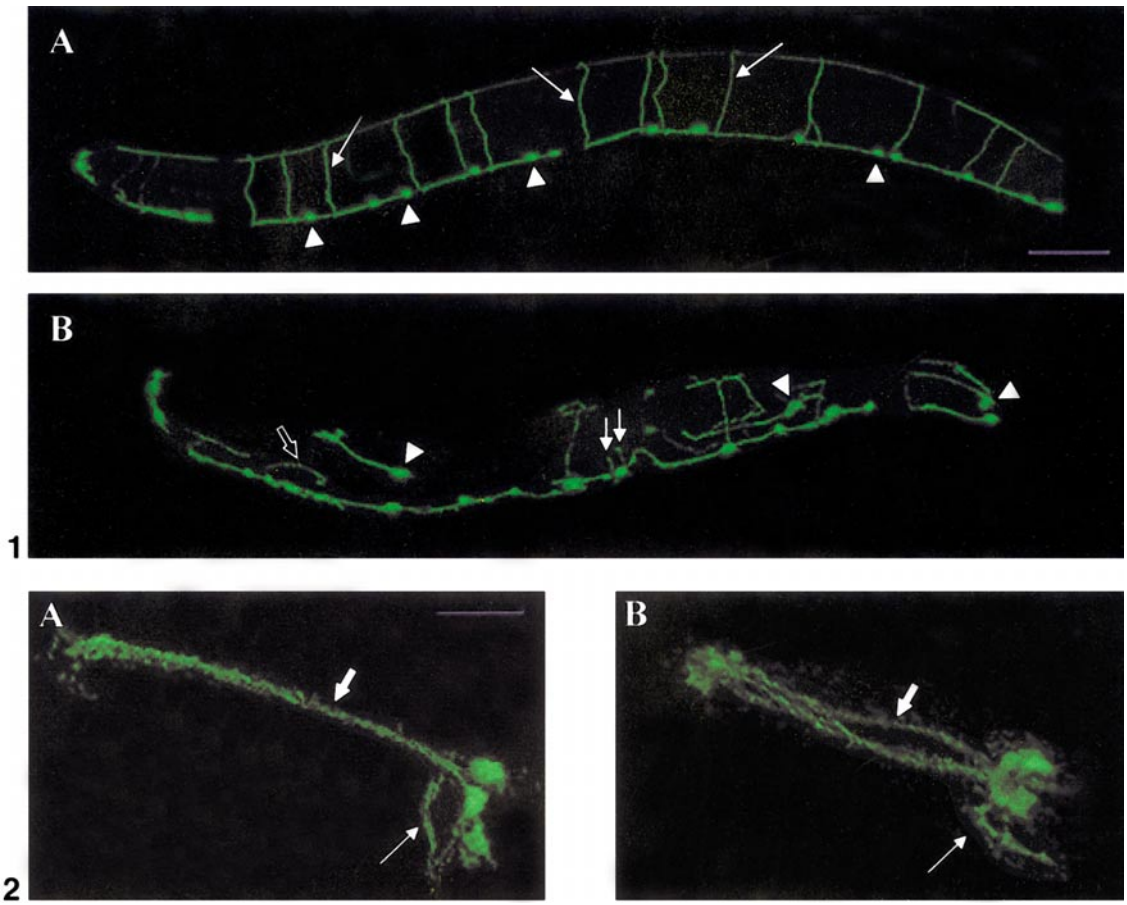

FIG. 1. Axons and cell bodies of D-type motoneurons in wild-type and *ced-10;mig-2* animals. (A) A photomicrograph of a wild-type worm carrying the *unc-25::gfp* transgene. The D-type motoneurons showed normal cell body positions (indicated by arrowheads) and commissure extensions (indicated by arrows). (B) A photomicrograph of a *ced-10*(*n1993*);*mig-2*(*mu28*) worm carrying the *unc-25::gfp* transgene. The animal was dumpy. Lateral VD neurons were indicated by arrowheads. Misrouting and premature termination of commissures are indicated by the open arrow and arrows, respectively. Both pictures are a projection of 20 serial confocal images. Dorsal is up and anterior is to the left. Scale bar, 40 μm.

FIG. 2. Amphid neurons in wild-type and *ced-10*(*n1993*);*mig-2*(*mu28*) animals. (A) A photomicrograph of a wild-type adult stained with DiO. Amphid neurons on the left side of animal were shown. Axons extending to sensillum and nerve ring are indicated by the thick and thin arrows, respectively. (B) A photomicrograph of a *ced-10;mig-2* adult stained with DiO. Amphid axons extending to sensillum were defasciculated (indicated by the thick arrow). Partial axon processes were misrouting and did not enter the nerve ring (indicated by the thin arrow). Both pictures are a projection of 20 serial confocal images. Dorsal is up and anterior is to the left. Scale bar, 20 μm.

commissures in all three *unc-73* alleles, *e936*, *gm33*, and *rh40* (Table 2).

UNC-73 contains two DH/PH domains and an SH3 motif located between two DH/PH domains. The exchange activities of GEFs are conferred by consecutive DH/PH domains (Habets *et al.*, 1995). Two such DH/PH domains exist in UNC-73 and are referred to here as GEF1 and GEF2. GEF1 and GEF2 have been shown to exhibit exchange activities toward mammalian Rac1 and RhoA, respectively (Spencer *et al.*, 2001). However, activities of these GEF domains toward *C. elegans* CED-10 and MIG-2 have not yet been studied. We therefore examined whether UNC-73 could physically interact with CED-10 and MIG-2 using the yeast two-hybrid system based on the DNA-binding domain (DB) and transactivation domain (AD) of the yeast GAL4 protein. In this system, an interaction between two tester proteins, one fused to DB and the other fused to AD, activates the expression of the GAL4-responsive reporter gene *HIS3* and allows yeast cells to grow on a plate lacking histidine (Bai and Elledge, 1997). In this experiment, we fused the UNC-73 GEF1/SH3 domain to the GAL4 DNA binding domain (DB) and CED-10, MIG-2, or CDC42 to the GAL4 activation domain (AD) and tested their interactions in the yeast strain MaV203 using the *HIS3* reporter gene. Interactions between UNC-73 GEF1/SH3 with CED-10 or MIG-2 but not CDC42 were observed in the yeast two-hybrid

TABLE 1

ced-10 and *mig-2* Act Redundantly to Control P Cell Migration and Axon Outgrowth of DD, VD, and Amphid Neurons

Genotype	% of animals with misplaced VD neurons[a]	% of animals with defect in DD and VD commissure outgrowth[a]	Amphid axon extension into the nerve ring[b,c]
ced-10(n1993)	2 (1.0 ± 0.0)	54 (1.9 ± 1.0)	+
ced-10(n3246)	4 (1.0 ± 0.0)	95 (3.8 ± 1.6)	+
mig-2(mu28)	0 (0.0 ± 0.0)	70 (2.4 ± 1.2)	+
ced-10(n1993);mig-2(mu28)	100 (4.8 ± 1.7)	100 (7.8 ± 2.0)	−

[a] Animals of indicated genotypes carrying the transgene *unc-25::gfp* (n = 50) were examined by using fluorescence microscopy. Parentheses indicate average numbers ± standard deviation of misplaced VD neurons or abnormal commissures observed in defective animals.

[b] Animals of indicated genotypes (n = 25 for *ced-10;mig-2*; n = 100 for other genotypes) were stained with DiO and observed by using fluorescence microscopy.

[c] +, Normal axon extension was observed in all animals examined; −, no axon extension into the nerve ring was observed in animals examined.

system (Fig. 3A), indicating that UNC-73 specifically interacts with CED-10 and MIG-2 *in vitro*.

We further tested whether UNC-73 GEF1/SH3 has a GEF activity for CED-10 or MIG-2 by using the [^{3}H]GDP release assay. We expressed an UNC-73 GEF1-MBP fusion protein and measured its ability to catalyze the release of [^{3}H]GDP from CED-10, MIG-2, and CDC42. We found that UNC-73GEF1-MBP fusion protein stimulated the release of [^{3}H]GDP specifically from CED-10 and MIG-2 but not CDC42 (Fig. 3B).

unc-73 Likely Acts Upstream of ced-10 and mig-2 during the Development of D Type Motoneurons and Amphid Sensory Neurons

To investigate whether *unc-73* may act through *ced-10* and *mig-2* to control P cell migration, we further examined the rescue effect of constitutively activated *ced-10* and *mig-2* on the P cell migration phenotype of *unc-73*(*rh40*) mutants. The *unc-73*(*rh40*) allele causes a missense mutation in the conserved DH1 domain and likely abolishes the GEF1 activity, as the equivalent mutation in the GEF1 domain eliminated its *in vitro* GEF activity for mammalian Rac (Steven *et al.*, 1998). We introduced the constitutively activated *mig-2* and *ced-10* in the *unc-73*(*rh40*) background using the gain-of-function *mig-2*(*gm38*) mutation and the heatshock-induced overexpression of the P_{hsp}*::ced-10(V12)* transgene, respectively (Zipkin *et al.*, 1997; Wu *et al.*, 2001). We found that both constitutively activated *mig-2* and *ced-10* significantly reduced the Unc-73 P cell migration defect (Table 3, and see below). Constitutively activated *mig-2* and *ced-10* decreased the percentage of *unc-73*(*rh40*) mutants with lateral VD neurons from 55 to 9 and 11%, respectively. The *mig-2*(*gm38*) mutation also greatly reduced the P cell migration phenotype of strong *unc-73*(*gm33*) mutants (Table 3). The *unc-73*(*gm33*) allele causes a point mutation in a splice consensus site and thus might encode a truncated protein without GEF1 and GEF2 do-

TABLE 2

unc-73 Acts with *ced-10* and *mig-2* to Control the Development of D-Type Motoneurons and Amphid Sensory Neurons

Genotype	% of animals with lateral VD neurons[a]	% of animals with defect in DD and VD commissure outgrowth[a]	Amphid axon extension into the nerve ring[b,c]
unc-73(e936)	35 (1.3 ± 0.6)	80 (2.5 ± 1.3)	+
unc-73(rh40)	55 (1.6 ± 1.0)	100 (3.6 ± 1.6)	+
unc-73(gm33)	100 (6.9 ± 1.8)	100 (7.0 ± 1.5)	−
unc-73(e936); ced-10(n3246)	70 (2.1 ± 2.3)	100 (4.8 ± 1.8)	+
unc-73(rh40); ced-10(n1993)	50 (1.4 ± 0.7)	100 (5.9 ± 1.9)	+
unc-73(e936); mig-2(mu28)	95 (3.3 ± 1.7)	100 (7.8 ± 2.1)	+/−
unc-73(rh40); mig-2(mu28)	100 (2.8 ± 1.5)	100 (7.8 ± 2.0)	−

[a] Animals of indicated genotypes carrying the transgene *unc-25::gfp* (n = 50) were examined by using fluorescence microscopy. Parentheses indicate average numbers ± standard deviation of lateral VD neurons or abnormal commissures observed in defective animals.

[b] Animals of indicated genotypes (n = 100) were stained with DiO and observed by using fluorescence microscopy.

[c] +, Normal axon extension was observed in all animals examined; −, no complete axon extension into the nerve ring was observed in animals examined; +/−, normal axon extension was observed in approximately 67% of animals examined.

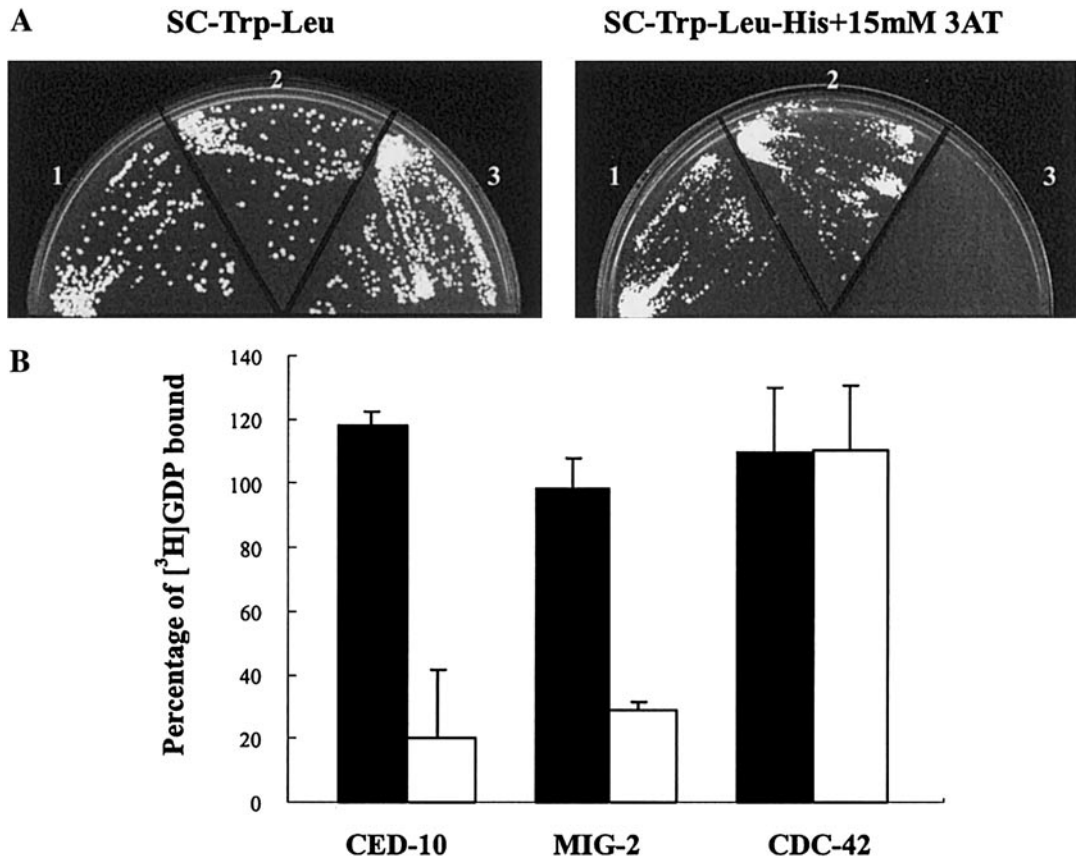

FIG. 3. UNC-73 interacts with CED-10 and MIG-2 and has GEF activity for CED-10 and MIG-2 *in vitro*. (A) UNC-73 GEF1/SH3 interacts with CED-10 and MIG-2 but not CDC42 in the yeast two-hybrid system. Constructs expressing indicated fusion proteins were transformed into the yeast strain MaV203 to generate respective transformants: (1) AD-CED-10 + DB-UNC-73, (2) AD-MIG-2 + DB-UNC-73, (3) AD-CDC-42 + DB-UNC-73. Resulting transformants were streaked on SC-Trp-Leu plates or SC-Trp-Leu-His plates + 15 mM 3AT. Growth on the latter plates indicates interaction of fusion proteins. (B) The GEF1 domain of UNC-73 has guanine nucleotide exchange activity specific for CED-10 and MIG-2 but not CDC42 *in vitro*. CED-10, MIG-2, and CDC42 were preloaded with [^{3}H]GDP and then incubated in the presence (white bars) or absence (black bars) of UNC-73GEF1-MBP fusion protein for 30 min. Amounts of bound [^{3}H]GDP after incubation were measured (see Materials and Methods). Results were obtained from four independent experiments.

mains (Steven *et al.*, 1998). Our genetic analysis suggests that *unc-73* likely acts upstream of *ced-10* and *mig-2* in a genetic pathway that controls P cell migration.

We also examined the rescue effect of constitutively activated *mig-2* and *ced-10* on the Unc-73 commissure outgrowth phenotype. The *mig-2*(*gm38*) mutation partially rescued the DD and VD commissure outgrowth defects in *unc-73*(*rh40*) mutants (Table 3). For example, 100% of *unc-73*(*rh40*) mutants exhibited on average 3.6 abnormal commissures, whereas approximately 39% of *unc-73*(*rh40*); *mig-2*(*gm38*)/+ mutants exhibited on average 1.6 defective commissures. Similarly, constitutively activated *ced-10(V12)* also greatly reduced the commissure outgrowth defects in *unc-73*(*e936*) and *unc-73*(*rh40*) mutants (Table 4). We heatshocked *unc-73*;P_{hsp}*::ced-10(V12)* animals at midembryos and scored the phenotype at early L1 to specifically examine the rescue effect on DD commissures, as extensive heatshock covering the developmental period of both DD and VD neurons somehow killed worms. Approximately 62% of heat-shocked *unc-73*(*rh40*) mutants and 14% of heat-shocked *unc-73*(*rh40*);P_{hsp}*::ced-10(V12)* animals displayed DD commissure outgrowth defects (Table 4). These results suggest that *unc-73* likely acts upstream of *mig-2* and *ced-10* during the commissure outgrowth of D-type motoneurons.

Interestingly, the loss-of-function mutation in either *mig-2* or *ced-10* significantly increases numbers of defective commissures in *unc-73*(*rh40*) mutants (Table 2). It is possible that an additional GEF besides UNC-73 GEF1 is involved in activation of CED-10 and MIG-2 during DD and VD commissure outgrowth. Alternatively, the UNC-73 GEF1 activity for CED-10 and MIG-2 may not be completely eliminated in *unc-73*(*rh40*) mutants. On the other hand, the *mig-2* but not *ced-10* mutation showed aggrava-

TABLE 3

Effects of the *mig-2(gm38)* Mutation on the Development of D-Type Motoneurons and Amphid Sensory Neurons in Different Genetic Backgrounds

Genotype[a]	% of animals with lateral VD neurons[b]	% of animals with defect in DD and VD commissure outgrowth[b]	Amphid axon extension into the nerve ring[c,d]
mig-2(gm38)/+	0 (0.0 ± 0.0)	16 (1.0 ± 0.0)	+
unc-73(gm33); mig-2(gm38)/+	53 (1.1 ± 0.3)	79 (1.9 ± 1.1)	+/−
unc-73(rh40); mig-2(gm38)/+	9 (1.0 ± 0.0)	39 (1.6 ± 0.8)	ND
ced-10(n1993); mig-2(gm38)/+	0 (0.0 ± 0.0)	27 (1.0 ± 0.0)	ND
ced-2(e1752); mig-2(gm38)/+	0 (0.0 ± 0.0)	18 (1.0 ± 0.0)	ND
ced-5(n1812); mig-2(gm38)/+	0 (0.0 ± 0.0)	25 (1.1 ± 0.4)	ND
ced-2(n1994) ced-10(n3246); mig-2(gm38)/+	0 (0.0 ± 0.0)	37 (1.4 ± 0.5)	ND
ced-10(n3246) ced-5(n1812); mig-2(gm38)/+	0 (0.0 ± 0.0)	42 (1.3 ± 0.6)	ND
ced-12(n3261); ced-10(n3246); mig-2(gm38)/+	0 (0.0 ± 0.0)	41 (1.4 ± 0.5)	ND

Note. ND, not determined.

[a] Strains contained an additional *lon-2/+* mutation to help distinguishing *mig-2(gm38)/+* heterozygous worms. Animals in the *mig-2(gm38)/+* heterozygous background are less defective in P cell migration and axon outgrowth than those in the *mig-2(gm38)* homozygous background (data not shown).

[b] Animals (n = 50) of indicated genotypes carrying the transgene *unc-25::gfp* were examined by using fluorescence microscopy. Parentheses indicate average numbers ± standard deviation of lateral VD neurons or abnormal commissures observed in defective animals.

[c] Animals (n = 100) of indicated genotypes were stained with DiO and observed by using fluorescence microscopy.

[d] +, Normal axon extension was observed in all animals examined; −, no complete axon extension into the nerve ring was observed in all animals examined; +/−, normal axon extension was observed in approximately 31% worms examined.

tion in the P cell migration defect in *unc-73*(*rh40*) mutants (Table 2). This suggests that MIG-2 but not CED-10 may require a GEF activity in addition to UNC-73 GEF1 during P cell migration.

ced-2 and ced-5 Likely Act through mig-2 but Not ced-10 to Regulate P Cell Migration

ced-2, *ced-5*, and *ced-12* have been shown to act through *ced-10* to control cell-corpse engulfment and DTC migration (Gumienny *et al.*, 2001; Wu *et al.*, 2001; Zhou *et al.*, 2001). We further explored whether these three genes play roles in other *ced-10*-mediated cellular processes, such as P cell migration. The mutations *ced-2*(*n1994*), *ced-5*(*n1812*), and *ced-12*(*n3261*) used in the experiments are likely null (Reddien and Horvitz, 2000; Zhou *et al.*, 2001). We found that *ced-2*, *ced-5*, and *ced-12* mutants appeared to have normal P cell migration based on the correct localization of VD neurons in the ventral cord (Table 5). However, the finding that mutations in *ced-2* or *ced-5* significantly enhanced the lateral VD phenotype in *ced-10* or *unc-73* mutants indicates that *ced-2* and *ced-5* likely act with *ced-10* and *unc-73* in a redundant way during P cell migration (Table 5). In contrast, like *mig-2*(*mu28*) mutants, *ced-2;mig-2*(*mu28*) and *ced-5;mig-2*(*mu28*) double mutants did not exhibit a P cell migration defect. These observations suggest that *ced-2* and *ced-5* likely act with *mig-2* in a genetic pathway to control P cell migration. Because *ced-2 ced-5* double mutants displayed normal P cell migration as their respective single mutants, *ced-2* and *ced-5* likely act in the same pathway during P cell migration. On the other hand, *ced-12* does not enhance the P cell migration phenotype of *ced-10*, *mig-2*, and *unc-73* mutants (Table 5). This observation suggests that *ced-12* is uncoupled from *ced-2* and *ced-5* and likely plays no role in P cell migration.

We further investigated whether *ced-2* and *ced-5* could act upstream of *mig-2* during P cell migration by testing whether the *mig-2*(*gm38*) mutation can rescue the P cell migration defect in *ced-2* or *ced-5* mutants. We performed this experiment in the *ced-10* background as *ced-2* or *ced-5*

TABLE 4

Effect of Constitutively Activated *ced-10* on DD Axon Outgrowth in Different Genetic Backgrounds

Genotype	Heat shock	% of animals with defect in DD axon outgrowth (n = 20)[a]
ced-10(n3246)	+	67
ced-10(n3246); P_{hsp}:: ced-10V12	+	22
ced-2(n1994)	+	18
ced-2(n1994); P_{hsp}:: ced-10V12	+	0
ced-5(n1812)	+	28
ced-5(n1812); P_{hsp}:: ced-10V12	+	0
ced-12(tp2)	+	8
ced-12(tp2); P_{hsp}:: ced-10V12	+	8
unc-73(e936)	+	17
unc-73(e936); P_{hsp}:: ced-10V12	+	4
unc-73(rh40)	+	62
unc-73(rh40); P_{hsp}:: ced-10V12	+	14

[a] Embryos of indicated genotypes carrying the transgene *unc-25::gfp* were heat shocked and scored for DD axon outgrowth by using fluorescence microscopy (see Materials and Methods).

TABLE 5
The Development of D-Type Motoneurons and Amphid Sensory Neurons in the *ced-2, ced-5,* and *ced-12* Strains

Genotype	% of animals with lateral VD neurons	% of animals with defect in DD and VD axon outgrowth[a]	Amphid axon extension into the nerve ring[b,c]
ced-2(e1752)	0 (0.0 ± 0.0)	48 (1.4 ± 0.7)	+
ced-2(n1994)	4 (1.0 ± 0.0)	67 (2.3 ± 1.5)	+
ced-2(e1752) ced-10(n3246)	18 (1.3 ± 0.5)	88 (3.4 ± 1.5)	+
ced-2(n1994) ced-10(n3246)	13 (1.1 ± 0.4)	91 (3.7 ± 1.8)	+
ced-2(e1752); mig-2(mu28)	0 (0.0 ± 0.0)	76 (2.4 ± 1.3)	+
ced-2(n1994); mig-2(mu28)	0 (0.0 ± 0.0)	77 (1.6 ± 0.9)	+
unc-73(e936); ced-2(e1752)	56 (1.5 ± 0.7)	98 (4.5 ± 1.9)	+
unc-73(e936); ced-2(n1994)	56 (1.6 ± 1.0)	98 (5.5 ± 2.0)	+
ced-5(n1812)	0 (0.0 ± 0.0)	64 (2.3 ± 1.4)	+
ced-5(n2002)	0 (0.0 ± 0.0)	66 (1.5 ± 0.7)	+
ced-10(n3246) ced-5(n1812)	16 (1.2 ± 0.5)	100 (3.9 ± 1.2)	+
ced-10(n3246) ced-5(n2002)	12 (1.0 ± 0.0)	100 (3.9 ± 2.2)	+
ced-5(n2002); mig-2(mu28)	0 (0.0 ± 0.0)	73 (2.1 ± 1.0)	+
unc-73(e936);ced-5(n1812)	60 (1.4 ± 0.6)	98 (4.7 ± 1.8)	+
unc-73(e936);ced-5(n2002)	59 (1.3 ± 0.4)	100 (5.5 ± 1.9)	+
ced-12(tp2)	0 (0.0 ± 0.0)	55 (2.0 ± 1.6)	+
ced-12(n3261)	0 (0.0 ± 0.0)	65 (1.7 ± 0.9)	+
ced-12(tp2); ced-10(n3246)	0 (0.0 ± 0.0)	75 (2.0 ± 1.1)	+
ced-12(n3261); ced-10(n3246)	3 (1.0 ± 0.0)	75 (1.8 ± 1.1)	+
ced-12(tp2); mig-2(mu28)	0 (0.0 ± 0.0)	84 (2.6 ± 1.0)	+
ced-12(n3261); mig-2(mu28)	0 (0.0 ± 0.0)	91 (2.3 ± 1.1)	+
unc-73(e936) ced-12(tp2)	28 (1.1 ± 0.4)	87 (3.1 ± 1.5)	+
unc-73(e936) ced-12(n3261)	ND	100 (3.7 ± 1.9)	+
ced-2(n1994) ced-5(n2002)	0 (0.0 ± 0.0)	67 (2.2 ± 1.3)	+

[a] Animals of indicated genotypes carrying the transgene *unc-25::gfp* ($n = 50$) were examined by using fluorescence microscopy. Parentheses indicate average numbers ± standard deviation of lateral VD neurons or abnormal commissures observed in defective animals.
[b] Animals of indicated genotypes ($n = 100$) were stained with DiO and observed by using fluorescence microscopy.
[c] +, Normal axon extension was observed in all animals examined.

mutants exhibited a P cell migration defect in the *ced-10* but not wild-type background. We found that *ced-2 ced-10*; *mig-2*(*gm38*)/+ and *ced-5 ced-10*;*mig-2*(*gm38*)/+ mutants showed a significantly reduced defect in P cell migration as compared with *ced-2 ced-10* and *ced-5 ced-10* mutants, respectively (Tables 3 and 5). Together, these findings suggest that *ced-2* and *ced-5* genetically act upstream of *mig-2* but not *ced-10* to control P cell migration (Fig. 4A).

ced-2 and ced-5 Likely Act Upstream of ced-10 and mig-2 to Control DD and VD Axon Outgrowth

We next examined whether *ced-2*, *ced-5*, and *ced-12* may play roles during the commissure outgrowth of DDs and VDs. We found that more than 50% of *ced-2*, *ced-5*, or *ced-12* mutants had mild defects in commissure outgrowth: on average, two commissures showed defects of pretermination, branching, or misrouting (Table 5). Mutations in either *ced-2* or *ced-5* enhanced the DD and VD commissure defects in the *unc-73* but not *ced-10* or *mig-2* background (Table 5). The *mig-2*(*gm38*) mutation and overexpression of the *hsp::ced-10(V12)* transgene partially suppressed the commissure defects in *ced-2* and *ced-5* mutants (Tables 3 and 4). Together, these results suggest that *ced-2* and *ced-5* may act redundantly with *unc-73* and upstream of *ced-10* and *mig-2* during DD and VD commissure outgrowth (Fig. 4B).

Intriguingly, mutations in *ced-12* slightly suppressed, but weakly enhanced, the DD and VD commissure outgrowth defects in *ced-10* and *mig-2(mu28)* mutants, respectively (Table 5). Heatshock-induced expression of the *hsp::ced-10(V12)* transgene appeared to have no rescue effect on the commissure outgrowth defects in *ced-12* mutants (Table 4), suggesting that *ced-12* might not act upstream of *ced-10* during commissure outgrowth. *ced-12; mig-2(mu28)* double mutants exhibited observable but very weak uncoordination in movement, which is not observed in *ced-12* or *mig-2(mu28)* single mutants. Thus, *ced-12* and *mig-2* may function redundantly during DD and VD commissure outgrowth.

Amphid Axon Extension Involves both GEF1 and GEF2 Activities of UNC-73 but Not CED-2, CED-5, and CED-12

Although *unc-73*(*rh40*) and *mig-2*(*mu28*) single mutants were normal in amphid axon outgrowth, *unc-73*(*rh40*);

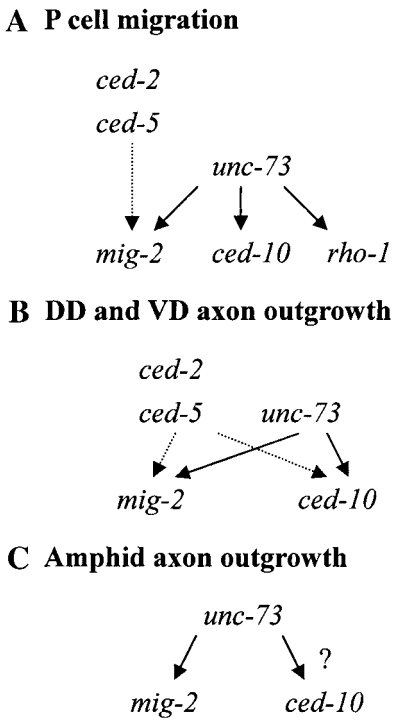

FIG. 4. Models for rac-mediated pathways during P cell migration and axon outgrowth of D type motoneurons and amphid sensory neurons. Broken arrows indicate a subtle function. (A) *ced-10*, *mig-2*, and *rho-1* likely act redundantly in P cell migration. *unc-73* acts in all three pathways. *ced-2* and *ced-5* likely act upstream of *mig-2* and in parallel to *ced-10* and *unc-73*. (B) *ced-10* and *mig-2* act redundantly in DD and VD axon outgrowth and may be regulated by at least two redundant pathways with *ced-2* and *ced-5* in one and *unc-73* in the other. (C) *ced-10* and *mig-2* act redundantly to control amphid axon extension into the nerve ring. *unc-73* likely acts upstream of *mig-2*. The genetic relationship between *unc-73* and *ced-10* has not been demonstrated. *ced-2*, *ced-5*, and *ced-12* are not involved.

mig-2(*mu28*) double mutants were defective in amphid axon development (Tables 1 and 2). This observation suggests that, in addition to MIG-2, UNC-73 GEF1 is involved in amphid axon outgrowth. UNC-73 GEF2 may also play a role during amphid axon outgrowth, as *unc-73*(*gm33*) but not *unc-73*(*rh40*) mutants were defective in amphid axon development (Table 2). The allele *rh40* affects only the GEF1 domain, whereas the *gm33* allele affects both GEF1 and GEF2 domains. The finding that the *mig-2*(*gm38*) mutation can partially rescue the defect of amphid axon outgrowth in *unc-73*(*gm33*) mutants suggests that *unc-73* may act upstream of *mig-2* to control amphid axon outgrowth (Fig. 4C). Because the heatshock treatment of *unc-73*(*gm33*); *hsp::ced-10(V12)* animals resulted in lethality (we have not yet examined the cause of lethality), we could not assess the genetic relationship between *unc-73* and *ced-10* during amphid axon outgrowth by the transcriptional overexpression method.

We further examined whether *ced-2*, *ced-5*, and *ced-12* are involved in amphid axon development. We found that *ced-2*, *ced-5*, and *ced-12* single mutants showed normal amphid axon extension and that *ced-2*, *ced-5*, and *ced-12* double mutants with *ced-10*, *mig-2*, or *unc-73* also did not display any observable defect in amphid axons (Table 5). These findings suggest that *ced-2*, *ced-5*, and *ced-12* likely play no role in amphid axon outgrowth. Therefore, alternative rac regulator(s) other than *ced-2*, *ced-5*, and *ced-12* are utilized to control amphid axon outgrowth.

DISCUSSION

We present models for the function of two *C. elegans* rac genes *ced-10* and *mig-2* and the pathways that lead to their activation in P cell migration and axon outgrowth of DDs, VDs, and amphid neurons. *ced-10*(*n1993*);*mig-2*(*mu28*) double mutants exhibit synthetic defects that are not observed in single mutants, such as dumpy body shape, lateral vulvae, high-rate lethality, small brood size, and uncoordinated movement, suggesting that *ced-10* and *mig-2* play redundant roles in many cellular processes (Lundquist *et al.*, 2001; Spencer *et al.*, 2001, and our observations). By analyzing D-type motoneurons and amphid sensory neurons in these mutants, we showed that *ced-10* and *mig-2* act redundantly during P cell migration and axon outgrowth of DDs, VDs, and amphid neurons (Fig. 4). Interestingly, although *ced-10*;*mig-2* mutants exhibited abnormal amphid axon outgrowth, their amphid dendrites appeared normal. This observation suggests that amphid neurons use distinct signaling pathways to control axon and dendrite formation.

Our biochemical data suggest that the GEF1 domain of UNC-73 has a guanine nucleotide exchange activity for both CED-10 and MIG-2 *in vitro*, consistent with the previous finding that the GEF1 domain of the *Drosophila* Trio acts on *Drosophila* Rac1 and *Drosophila* Mtl (MIG-2 like) (Newsome *et al.*, 2000). RHO-1 has been shown to function in P cell migration, likely through activation by UNC-73 GEF2 (Spencer *et al.*, 2001). Thus, UNC-73 likely functions as a common exchange factor for CED-10, MIG-2, and RHO-1 during P cell migration, with the GEF1 domain acting on CED-10 and MIG-2 and the GEF2 domain on RHO-1 (Fig. 4A). UNC-73, CED-10, and MIG-2 also act in axon outgrowth of D-type motoneurons (Fig. 4B) and amphid sensory neurons (Fig. 4C). Biochemical data and genetic analyses suggest that UNC-73 likely activates CED-10 and MIG-2 through the GEF1 domain to control the axon outgrowth of D-type motoneurons and amphid sensory neurons (Figs. 4B and 4C). Genetic analysis indicates that UNC-73 GEF2 likely functions in these axonal outgrowth processes as well. For example, axon outgrowth defects of *unc-73*(*gm33*) mutants are more severe than those of *unc-73*(*rh40*) mutants (Table 2). The *rh40* mutation abolishes UNC-73 GEF1 activities for RAC, and the *gm33* mutation affects both GEF1 and GEF2 domains of UNC-73 (Steven *et al.*, 1998). Previous biochemical assay showed

that UNC-73 GEF2 had a GEF activity for human RhoA but not RAC (Spencer *et al.*, 2001). Therefore, UNC-73 GEF2 probably act through *rho-1* but not *ced-10* or *mig-2* to control axon outgrowth of DDs, VDs, and amphid neurons. An additional GEF besides UNC-73 may be important for the activation of CED-10 and MIG-2 during the axon outgrowth of DDs, VDs, and amphid neurons, as defects in these axon outgrowths in *unc-73*(*rh40*) mutants are not as severe as those in *unc-73*(*rh40*);*mig-2(mu28)*, *unc-73*(*rh40*); *ced-10*, and *ced-10;mig-2(mu28)* double mutants. Therefore, multiple GEFs may regulate various GTPase activities during the development of DD, VD, and amphid axons.

Previous genetic and biochemical studies showed that *ced-2*, *ced-5*, and *ced-12* mediate signaling that leads to *ced-10* activation during the phagocytosis of apoptotic cells (Gumienny *et al.*, 2001; Wu *et al.*, 2001; Zhou *et al.*, 2001). We found that *ced-2*, *ced-5*, and *ced-12* were not required in some *ced-10*-mediated pathways as our genetic data showed that *ced-2*, *ced-5*, and *ced-12* play no role during amphid axon outgrowth. Moreover, we showed that *ced-12* can be uncoupled from *ced-2* and *ced-5* in some rac-dependent developmental processes, as our genetic data indicate that *ced-2* and *ced-5* but not *ced-12* are involved in P cell migration. Similarly, *ced-2* has been shown to be uncoupled from *ced-5* during CAN axon pathfinding and CAN cell migration (Lundquist *et al.*, 2001). On the other hand, *ced-2* and *ced-5* appear to activate *ced-10* and *mig-2* differentially in various cellular processes, as *ced-2* and *ced-5* preferentially activate *ced-10* and *mig-2* during cell-corpse engulfment (Reddien and Horvitz, 2000) and P cell migration, respectively, but activate both *ced-10* and *mig-2* activities during DD and VD commissure outgrowth. Both *ced-10* and *mig-2* appear to be broadly expressed (Zipkin *et al.*, 1997; Reddien and Horvitz, 2000). Therefore, upon stimulation of extracellular signals, distinct upstream rac regulators but not differential expressions of rac molecules likely play major roles in the specific cellular responses of migrating cells and developing neurons.

ACKNOWLEDGMENTS

We thank J. Culotti and R. Steven for the *unc-73* minigene, Andy Fire for the *myo-2::gfp* construct, and Y. Kohara for *mig-2*, *cdc-42*, and *unc-73* cDNA clones. We thank J. Culotti, G. Garriga, H. R. Horvitz, Y. Jin, and the *Caenorhabditis* Genetics Center, which is funded by the NIH National Center for Research resources (NCRR), for providing *Caenorhabditis* strains. The confocal scanning microscope and some equipment used in this research were provided by core laboratories of Program for Promoting Academic Excellence of Universities. This research was supported in part by Ministry of Education Grant 89-B-FA01-1-4 and the National Science Council.

REFERENCES

Awasaki, T., Saito, M., Sone, M., Suzuki, E., Sakai, R., Ito, K., and Hama, C. (2000). The *Drosophila* trio plays an essential role in patterning of axons by regulating their directional extension. *Neuron* **26,** 119–131.

Bai, C., and Elledge, S. J. (1997). Gene identification using the yeast two-hybrid system. *Methods Enzymol.* **273,** 331–347.

Brenner, S. (1974). The genetics of *Caenorhabditis elegans*. *Genetics* **77,** 71–94.

Debant, A., Serra-Pages, C., Seipel, K., O'Brien, S., Tang, M., Park, S. H., and Streuli, M. (1996). The multidomain protein Trio binds the LAR transmembrane tyrosine phosphatase, contains a protein kinase domain, and has separate rac-specific and rho-specific guanine nucleotide exchange factor domains. *Proc. Natl. Acad. Sci. USA* **93,** 5466–5471.

D'Souza-Schorey, C., Boshans, R. L., McDonough, M., Stahl, P. D., and Van Aelst, L. (1997). A role for POR1, a Rac1-interacting protein, in ARF6-mediated cytoskeletal rearrangements. *EMBO J.* **16,** 5445–5454.

Gumienny, T. L., Brugnera, E., Tosello-Trampont, A. C., Kinchen, J. M., Haney, L. B., Nishiwaki, K., Walk, S. F., Nemergut, M. E., Macara, I. G., Francis, R., Schedl, T., Qin, Y., Van Aelst, L., Hengartner, M. O., and Ravichandran, K. S. (2001). CED-12/ELMO, a novel member of the CrkII/Dock180/Rac pathway, is required for phagocytosis and cell migration. *Cell* **107,** 27–41.

Habets, G. G., van der Kammen, R. A., Stam, J. C., Michiels, F., and Collard, J. G. (1995). Sequence of the human invasion-inducing TIAM1 gene, its conservation in evolution and its expression in tumor cell lines of different tissue origin. *Oncogene* **10,** 1371–1376.

Hall, A. (1998). Rho GTPases and the actin cytoskeleton. *Science* **279,** 509–514.

Hardt, W. D., Chen, L. M., Schuebel, K. E., Bustelo, X. R., and Galan, J. E. (1998). *S. typhimurium* encodes an activator of Rho GTPases that induces membrane ruffling and nuclear responses in host cells. *Cell* **93,** 815–826.

Hedgecock, E. M., Culotti, J. G., Thomson, J. N., and Perkins, L. A. (1985). Axonal guidance mutants of *Caenorhabditis elegans* identified by filling sensory neurons with fluorescein dyes. *Dev. Biol.* **111,** 158–170.

Herman, R. K., and Hedgecock, E. M. (1990). Limitation of the size of the bulval primordium of *Caenorhabditis elegans* by *lin-15* expression in surrounding hypodermis. *Nature* **348,** 169–171.

Jin, Y., Jorgensen, E., Hartwieg, E., and Horvitz, H. R. (1999). The *Caenorhabditis elegans* gene *unc-25* encodes glutamic acid decarboxylase and is required for synaptic transmission but not synaptic development. *J. Neurosci.* **19,** 539–548.

Kaibuchi, K., Kuroda, S., and Amano, M. (1999). Regulation of the cytoskeleton and cell adhesion by the Rho family GTPases in mammalian cells. *Annu. Rev. Biochem.* **68,** 459–486.

Liebl, E. C., Forsthoefel, D. J., Franco, L. S., Sample, S. H., Hess, J. E., Cowger, J. A., Chandler, M. P., Shupert, A. M., and Seeger, M. A. (2000). Dosage-sensitive, reciprocal genetic interactions between the Abl tyrosine kinase and the putative GEF trio reveal trio's role in axon pathfinding. *Neuron* **26,** 107–118.

Lundquist, E. A., Reddien, P. W., Hartwieg, E., Horvitz, H. R., and Bargmann, C. I. (2001). Three *C. elegans* Rac proteins and several alternative Rac regulators control axon guidance, cell migration and apoptotic cell phagocytosis. *Development* **128,** 4475–4488.

McIntire, S. L., Jorgensen, E., Kaplan, J., and Horvitz, H. R. (1993). The GABAergic nervous system of *Caenorhabditis elegans*. *Nature* **364,** 337–341.

Newsome, T. P., Schmidt, S., Dietzl, G., Keleman, K., Asling, B., Debant, A., and Dickson, B. J. (2000). Trio combines with dock to

regulate Pak activity during photoreceptor axon pathfinding in *Drosophila*. *Cell* **101,** 283–294.

O'Brien, S. P., Seipel, K., Medley, Q. G., Bronson, R., Segal, R., and Streuli, M. (2000). Skeletal muscle deformity and neuronal disorder in Trio exchange factor-deficient mouse embryos. *Proc. Natl. Acad. Sci. USA* **97,** 12074–12078.

Reddien, P. W., and Horvitz, H. R. (2000). CED-2/CrkII and CED-10/Rac control phagocytosis and cell migration in *Caenorhabditis elegans*. *Nat. Cell Biol.* **2,** 131–136.

Settleman, J. (2001). Rac 'n Rho: The music that shapes a developing embryo. *Dev. Cell* **1,** 321–331.

Spencer, A. G., Orita, S., Malone, C. J., and Han, M. (2001). A RHO GTPase-mediated pathway is required during P cell migration in *Caenorhabditis elegans*. *Proc. Natl. Acad. Sci. USA* **98,** 13132–13137.

Steven, R., Kubiseski, T. J., Zheng, H., Kulkarni, S., Mancillas, J., Ruiz Morales, A., Hogue, C. W., Pawson, T., and Culotti, J. (1998). UNC-73 activates the Rac GTPase and is required for cell and growth cone migrations in *C. elegans*. *Cell* **92,** 785–795.

Sulston, J. E. (1976). Post-embryonic development in the ventral cord of *Caenorhabditis elegans*. *Philos. Trans. R. Soc. Lond. B Biol. Sci.* **275,** 287–297.

White, J. G., Southgate, E., Thomson, J. N., and Brenner, S. (1986). The structure of the nervous system of the nematode *Caenorhabditis elegans*. *Philos. Trans. R. Soc. Lond. B Biol. Sci.* **314,** 1–340.

Wu, Y. C., and Horvitz, H. R. (1998). *C. elegans* phagocytosis and cell-migration protein CED-5 is similar to human DOCK180. *Nature* **392,** 501–504.

Wu, Y. C., Tsai, M. C., Cheng, L. C., Chou, C. J., and Weng, N. Y. (2001). *C. elegans* CED-12 acts in the conserved crkII/DOCK180/Rac pathway to control cell migration and cell corpse engulfment. *Dev. Cell* **1,** 491–502.

Zhou, Z., Caron, E., Hartwieg, E., Hall, A., and Horvitz, H. R. (2001). The *C. elegans* PH domain protein CED-12 regulates cytoskeletal reorganization via a Rho/Rac GTPase signaling pathway. *Dev. Cell* **1,** 477–489.

Zipkin, I. D., Kindt, R. M., and Kenyon, C. J. (1997). Role of a new Rho family member in cell migration and axon guidance in *C. elegans*. *Cell* **90,** 883–894.

Received for publication March 20, 2002
Revised July 2, 2002
Accepted July 11, 2002
Published online August 26, 2002